

# Nanocomposite Dielectric Elastomer Actuator for Micropump Diaphragms- Material Fabrication and Simulation Studies

Adithya Lenin<sup>1,2</sup>, Pandurangan Arumugam<sup>1</sup>

<sup>1</sup>Dept. of Chemistry, College of Engineering-Guindy, Anna University, Chennai, India

<sup>2</sup>Department of Mechanical Engineering, University of Iowa, Iowa City, IA 52242, USA

## Abstract

Electroactive polymers are a class of materials that deform when an electric field is applied. Dielectric elastomers are classified under electroactive polymers that are capable of producing very large deformations and this is due to their elastomeric nature. The fabrication of a dielectric elastomeric actuator based on a polymer nanocomposite with ceramic fillers is reported here. Polydimethylsiloxane (PDMS) was the choice of dielectric elastomer and hexagonal boron nitride (hBN) was used as dielectric fillers, which was added in weight percentages to the polymer. An amorphous carbon-filled polyvinyl acetate composite was used as the compliant electrode. Altering the stiffness of the polymer gives the ability to bring about small actuations, achieved by adding nanofillers to the polymer matrix. The incorporation of hBN into the matrix increased the tensile modulus of the pure PDMS from 0.297 MPa to a maximum of 0.535 MPa with a marginal rise in tensile strength. Scanning electron microscopy and elemental mapping were carried out to understand the morphology and filler distribution in the nanocomposites. From the experiments, the actual voltage (in kV) which was necessary to induce visible actuations in the nanocomposites was determined. Data from the experiments were used in the simulation studies. Finite element analysis was performed on the diaphragm model to predict the behavior of the material and active area displacement of the diaphragm was 1 mm at 8 kV, and deformation of 78 % was achieved. The simulation studies showed that the nanocomposite was perfectly suitable to be used as a pumping mechanism in micropumps.

**Keywords:** Actuator, Electroactive polymer, Finite element analysis, Nanocomposite, Micropump

## 1. Introduction

An actuator is a mechanism that converts one form of energy to another. There are several types of actuators based on pneumatics, piezoelectrics<sup>1</sup>, hydraulics, shape-memory alloys<sup>2</sup>, and electroactive polymers<sup>3</sup>, which can be used for specific functions, with each type having its merits and demerits. The most well-known one is the electromagnetic motor where electricity is used to perform mechanical motions, viz. rotate the blades of a ceiling fan or rotate an engine crankshaft in the case of a starter motor. In both these examples, the electric potential is converted to rotary mechanical work. Microactuators are devices that typically have actuations in the range of a few nanometers to millimeters<sup>4</sup>. These actuators are commonly used in micropumps, microvalves<sup>5</sup>, and switches.

Dielectric Elastomer Actuators (DEA) are parallel plate capacitors where a dielectric polymer is placed between two electrodes. Actuation here takes place when these coated electrodes trap the charges flowing through the device. Here the supplied voltage is converted into mechanical actuations. These actuations are based on a phenomenon known as electrostriction. Such polymers are known as electroactive polymers (EAP). The trapped electrons tend to deform the polymer causing the perceived actuation. EAPs produce very large strains almost around 100% or more<sup>6,7</sup> and are energy dense materials<sup>8</sup> and have values around  $1.63 \text{ J/cm}^3$  for silicone polymers and  $4 \text{ J/cm}^3$  for acrylic polymers<sup>9</sup>. However, for this to happen the Maxwell stress or electrostatic pressure generated by the electrodes must be greater than or equal to the elastic modulus of the material. Such strains are not possible in metals and these polymers weigh less<sup>10-12</sup>, which gives them an edge over conventional actuator materials. Based on the actuating mechanism EAPs are broadly classified into electronic<sup>13</sup> and ionic EAPs<sup>14</sup>. This paper deals with an electronic EAP actuator. Commonly used electronic EAPs are acrylic, silicone polymers<sup>15</sup>, polyurethanes, and various other copolymers<sup>8</sup>. Out of these, commercial acrylic elastomers<sup>17-22</sup> such as 3M™ VHB™ tape and silicones<sup>23-26</sup> are extensively studied owing to their ability to produce strains up to 100%<sup>13</sup>. The typical advantages of electronic EAPs over conventional actuator materials are their rapid response, large displacements, and ability to retain the deformed shape<sup>27</sup>. However, one of the major drawbacks of electronic EAPs is that they require very high actuation voltages, typically in kilovolts. Whereas ionic EAPs require very small actuation potential, in

order of volts. Although, the major limitation of ionic EAPs is that it requires an aqueous medium and salts to operate effectively<sup>28</sup>.

The well-known area of application for DEAs is in the biomedical realm. DEA-based artificial muscles could be used as implants to replace damaged muscle tissues to bring back their original function. Artificial muscles based on silicone and polyurethanes are the best choice as they are inert and biocompatible<sup>29-31</sup>. Apart from biomedical applications, these materials could also be used in sensors, energy storage devices<sup>32,33</sup>, and robotics<sup>16,34,35</sup>. This paper focuses on the application of the proposed material in microfluidics. Microfluidics deals with the flow control of very low volume fluids in the order of microliters. To transport such low volumes at a controlled flow rate<sup>36</sup>, specialized devices known as micropumps are required. EAPs could be useful in fabricating actuation mechanisms for micropumps to be used in microfluidic applications<sup>37</sup>. In micropumps and microvalves, the actuation mechanism is based on either electrostatics, piezoelectrics<sup>38</sup>, electromagnetics<sup>39</sup>, electrothermal<sup>40</sup>, or conducting polymers<sup>41</sup>. Since micropumps are used to transport very small volumes of fluids<sup>42,43</sup>, EAPs producing large-scale actuations must be avoided. Else, it would be very difficult to maintain control over such small volumes. The need for a low straining actuator with the attractive properties of electronic EAPs was the main motivation for developing this nanocomposite EAP. The material was made in such a way that it only produced tiny actuations and these tiny displacements would find application in the precise pumping of small volume liquids. The actuation mechanism here is a diaphragm that would displace fluids mechanically when supplied with an actuating voltage. Apart from microfluidics, there is a need for very precise actuations in the field of space optics to position mirrors and associated components. The James Webb telescope has actuators that are capable of making very small actuations in the order of nanometers<sup>44,45</sup>.

Herein a dielectric polymer nanocomposite was fabricated and its performance as a micropump diaphragm was analyzed. The nanocomposite was fabricated out of hBN and PDMS. PDMS is a highly elastic polymer that is often used in microfluidic devices<sup>46,47</sup>. It also facilitates the formation of thin films. Electrodes play a very crucial role in DEAs, the electrode material itself must be compliant i.e. it should be flexible and should have some electrical conductivity. These two parameters must be strictly

followed. Electrode materials are usually carbon-based greases<sup>48-50</sup> and metallic powders<sup>51-54</sup>. Initially, the choice of electrodes for this work were carbon-based grease and metallic silver paste. Based on experiments it was found that carbon grease electrodes were only suitable for stationary experiments and they break contact easily owing to their slippery nature. It was very hard to maintain sustained contact between the actuator material and the terminals. Silver paste electrodes applied on either side of the dielectric polymer nanocomposite were impractical and this observation was also made by other researchers<sup>55</sup>. It had very low resistance, and began conducting electricity, because of this no electrostriction occurred, and hence no actuation. To overcome these issues, we fabricated our composite electrodes using amorphous carbon black and polyvinyl acetate. Both PDMS and polyvinyl acetate are mutually compatible with each other i.e. the electrodes do not peel off when applied over the hBN-PDMS actuator. All the materials used in this work are cost-effective and readily available.

Stiffness in EAPs can open up many different avenues for it to be used in, but conventional stiffening methods are bulky and intricate<sup>56</sup>. The novelty of the material is its simplicity and ability to perform small controllable actuations, realized by tweaking the stiffness by adding hBN nanofillers to the polymer matrix. The nanofillers increased the breakdown strength of the material. Hexagonal BN has low dielectric permittivity and a high bandgap. The incorporation of hBN into the polymer increased its Young's modulus or elastic modulus. The increase in tensile modulus shows that the material became stiff. Thus, making it possible to produce small actuations.

A filler with high dielectric permittivity would help in lowering the driving voltage but the dielectric strength of the actuator would also be low, and device reliability cannot be guaranteed. In a previous study, the dielectric permittivity of the nanocomposite was altered with silicone oil, where BaTiO<sub>3</sub> a very high dielectric constant filler was used<sup>6</sup>. TiO<sub>2</sub> was also used as nanofillers to change the permittivity of the composite<sup>57</sup>. Carbon nanotubes, BNNTs<sup>58</sup> and lead titanate were also used as fillers to alter the electrical properties<sup>59</sup>. Although we have considerable expertise in working with BNNTs, here we opted to use hBN nanoparticles to reduce the final cost of the actuator. By using hBN, a sturdy nanocomposite actuator was fabricated, with a breakdown strength of 16 kV and a driving voltage of 8 kV.

Finite Element Analysis (FEA) helped in visualizing the working of the diaphragm actuator. Experimental data were used in the simulations. COMSOL Multiphysics ver. 5.5 software was used to perform the FEA simulations and actuators were designed in Solidworks 2014. The nanocomposite actuator showed promising actuation results.

## 2. Theory

The actuations in an EAP are based on electromechanics<sup>60-62</sup>. The exact working principle is electrostriction<sup>63,64</sup> along with the Maxwell stresses<sup>61,65-67</sup> which are generated when the flowing charges across the parallel plate device are restrained via a dielectric medium. These stresses are the main driving force for the actuations made. Here hBN was added to the EAP to increase the overall relative permittivity or dielectric constant of PDMS.

When the flowing charges are restricted by the dielectric medium, hBN-PDMS nanocomposite in this case, there is a build-up of charges across both electrodes, the trapped charges on either side of the electrodes attract or repel each other, thus bringing about some kind of deformation. Based on the placement of electrodes, and dielectric permittivity of the material used, actuations can be manipulated as required. In Fig.1, the 3D models of the common actuator types with electrodes are shown.

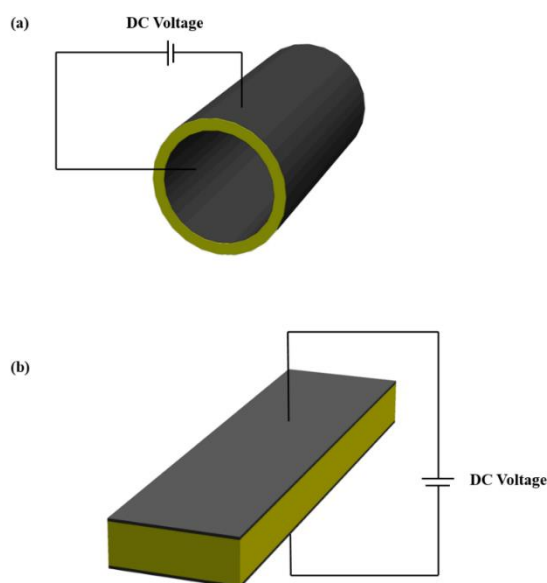


**Figure 1** Types of EAP actuators (a) Cylindrical (b) Cantilever beam

When a potential is applied between the electrodes, due to its dielectric nature an electrostrictive pressure or Maxwell stress is generated. This pressure compresses the EAP, which undergoes deformation based on electrode position. This is given by the equation<sup>68,69</sup>:

$$P = \epsilon_0 \epsilon_r \left[ \frac{V}{d} \right]^2 \quad (1)$$

Here  $v$  is the voltage applied across the electrodes and  $d$  is the thickness of the dielectric polymer. With this equation, the pressure generated for an applied voltage can be calculated in Pascal. However, this equation does not include the parameters of the compliant electrodes.

Since the actuator is a capacitance-based device, capacitance is given by the following equation:

$$C = \epsilon_0 \epsilon_r A / d \quad (2)$$

Where  $\epsilon_r$  is the relative permittivity of the material,  $\epsilon_0$  is the permittivity of vacuum which is a constant, the area of the dielectric medium is  $A$ , and the distance between the parallel plates is  $d$ . The device is a dielectric capacitor, electrostatic energy stored in it is given by,

$$U = Q^2 / 2C \quad (3)$$

Or

$$U = Q^2 d / 2 \epsilon_0 \epsilon_r A \quad (4)$$

Equation (4) is derived by substituting Eqn. (2) in Eqn. (3). The electrostatic pressure generated tends to deform the material by compressing it, thus differential changes are observed in the area ( $\delta A$ ) and thickness ( $\delta d$ ) of the material. However, the volume remains conserved. The strain produced is given by<sup>70</sup>,

$$S_z = -P/E \quad (5)$$

Or

$$S_z = -(\epsilon_0 \epsilon_r \left[ \frac{V}{d} \right]^2) / E \quad (6)$$

Where  $S_z$  is the strain along the z-axis of the planar surface and  $P$  is the electrostatic pressure. The elastic modulus of the material,  $E$ , is obtained from tensile test experiments. The negative sign indicates compression. In this work, the strain produced is small hence planar strains  $S_x$  and  $S_y$  are the same as there is uniform expansion along both axes due to the compression along the z-axis. Therefore,  $S_z$  is given as,

$$S_x = S_y = -0.5S_z \quad (7)$$

### 3. Experimental methods and characterizations

#### 3.1 Materials

The actuator was fabricated out of commercially available room temperature vulcanizing single part Anabond silicone/PDMS adhesives. For the sake of differentiation between the the nanocomposite actuator and pure PDMS actuator specimens, a red-dyed variant of the PDMS silicone adhesive was used to fabricate the nanocomposite actuator, namely the Anabond RTV Red silicone sealant. Pure PDMS actuator specimens were made using an undyed transparent variant of the same silicone adhesive viz. Anabond 666 RTV silicone sealant.

Hexagonal boron nitride was purchased from Ultrananotech Pvt. Ltd., India, and used as it is. Carbon black (amorphous) purchased from Merck, India, and commercial Polyvinyl Acetate (PVA) adhesive purchased from Pidilite Industries, India were used to fabricate the electrodes.

#### 3.2 Actuators and Electrode Fabrication

Ten grams of PDMS was taken and dissolved in n-hexane. The solution was sonicated until PDMS dissolved completely. Then the solution was syringe casted over a clean Polyethylene terephthalate (PET) sheet and was spread evenly. To avoid bubble formation, the sheet was placed in an air oven set at 30 °C for slow curing. After 24 hours, the PET sheet was taken out and the PDMS film was extracted from it by immersing the entire PET sheet in a trough containing n-hexane.

During this immersion process, PDMS absorbed the solvent and began to swell, this released the PDMS from the PET sheet. The peeled-off PDMS film was then placed in the oven set at 30 °C. PDMS film regained its original size after the solvent evaporated. The same procedure was followed for fabricating the nanocomposite specimens, except here, hBN filler was added in weight percentage. Two different nanocomposites with 2.5 wt. % hBN and 5 wt. % hBN were fabricated. The actuator material was trimmed to size as required for the experiments. A schematic of the nanocomposite fabrication process is given in Fig.2.

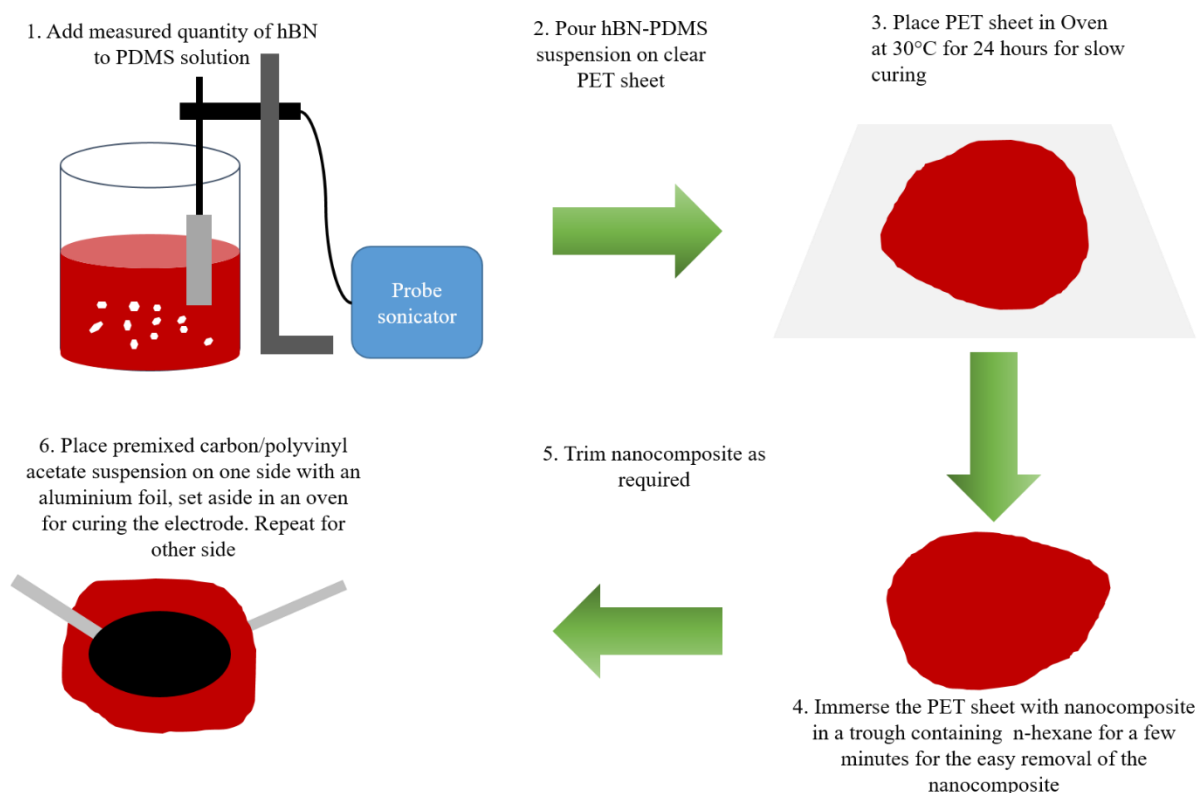


**Figure 2** Schematic of actuator fabrication

For electrode fabrication, PVA was mixed with a measured quantity of amorphous carbon black. Five grams of PVA was taken and dissolved in hot distilled water to get a homogenous solution and then 0.125 grams of amorphous carbon was added to the solution to make it conductive. The solution was then sonicated for 30 minutes. This suspension was carefully placed at different positions on the trimmed composite actuator. Thin strips of aluminium foil were used to create contact terminals. It was then placed in the oven at 50 °C for complete evaporation of water. The same was repeated for

the other side of the actuator. Fig. 3(a-d) shows the pure resin actuator and nanocomposite actuators with electrodes and terminals.

For experimental and testing purposes the actuators were designated as R1 (pure resin), BN1 (2.5 wt. % hBN), BN2 (5 wt. % hBN), and BD\* (5 wt. % hBN). BD\* denotes the actuator used for demonstrating the breakdown strength. Areas of both BN1 and BN2 were calculated and found to be similar.

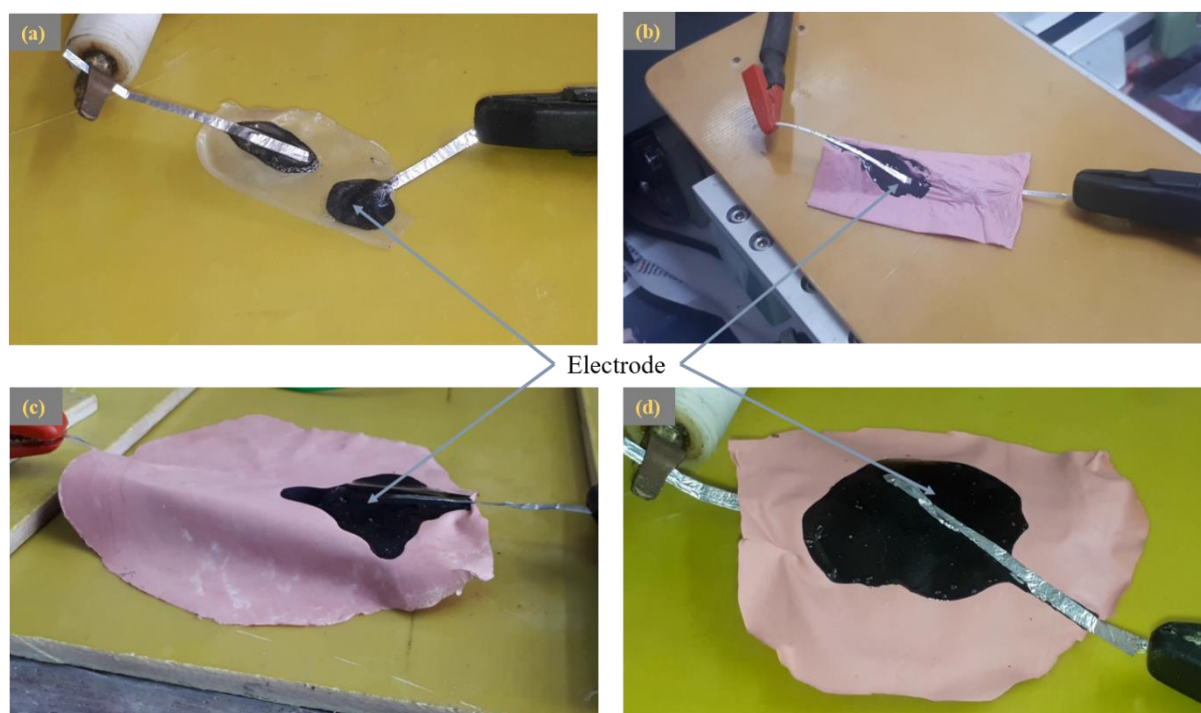


**Figure 3** Fabricated actuators and their designation (a) R1 (b) BD\* (c) BN1 (d) BN2

### 3.3 Experimental Setup and Characterization

TESCAN VEGA 3 scanning electron microscope (SEM) was used to study morphology in the hBN-PDMS nanocomposite. Additionally, elemental mapping was employed to confirm filler presence in the PDMS matrix. Dielectric permittivity of the nanocomposite was studied using a Keysight E4990A impedance analyzer at ambient room temperature.

Tensile tests were carried out according to the ASTM D882 standard. The tensile strength of both PDMS resin and nanocomposite was determined using the Tinius Olsen Universal Testing

Machine (UTM). Thin strips of 10 X 1 cm were cut out from the cured PDMS resin and nanocomposite sheets. The length of the samples under each category was 100 mm. The average thickness of the samples was 0.580 mm for both pure resin and nanocomposite films. The gauge length was set at 80 mm. The crosshead speed was set at 100mm/min.

A high voltage DC power supply unit (range 0- 40 kV) was employed to observe and study the displacements in the actuators and to obtain the actuation voltages, which were needed for the simulation studies. The actuators were then connected to a high voltage DC power supply unit and voltage was increased in a stepwise manner until actuations were observed. The experimental setup is shown in Fig. 4.

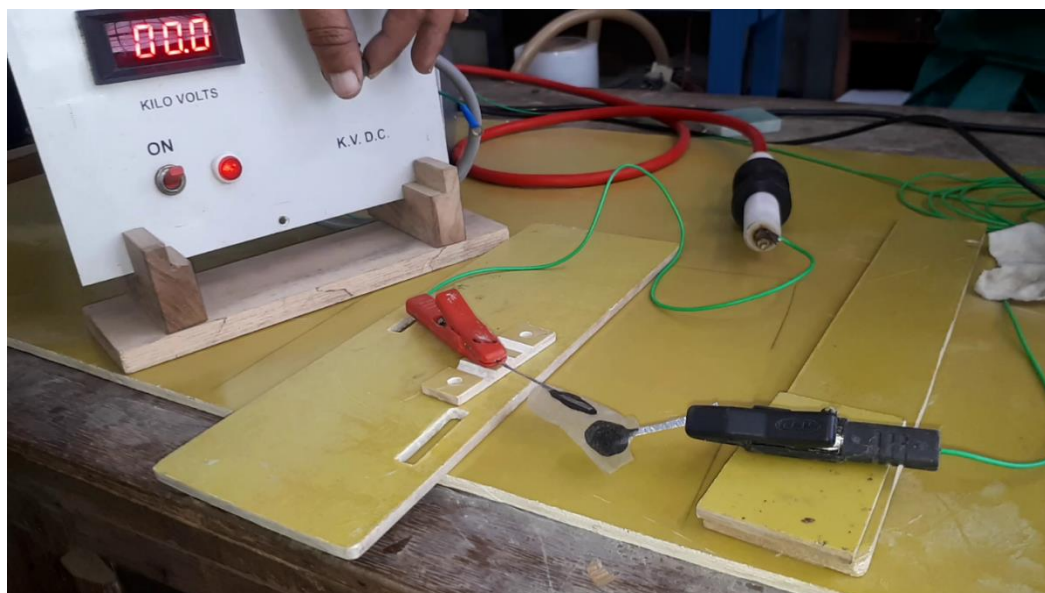


**Figure 4** The experimental setup for actuator testing shown along with DC power supply

## 4. Results and Discussion

### 4.1 Nanocomposite Actuator Materials

The SEM morphology of the BN1 and BN2 nanocomposite actuators are shown in Fig. 5(a) and 6(a). Figure 7(a) shows the morphology of the nanocomposite electrode with 2.5 wt. % of carbon added to polyvinyl acetate (PVA). It is to be noted that there is a substantial difference in filler content. As for the composite electrode, closeness among the carbon particles in the polymer matrix can be observed.

In Fig.5 (b-e) and Fig.6 (b-e), elemental maps of the BN1 and BN2 composite actuators are given. In BN1 and BN2, it should be noted that there is an even distribution of hBN among the polymer matrix.

In Fig. 7 (b-c), the elemental maps of the amorphous carbon-polyvinyl acetate composite are shown. Carbon and oxygen are the main elements in this polymer and also there is amorphous carbon, all can be seen in the maps.

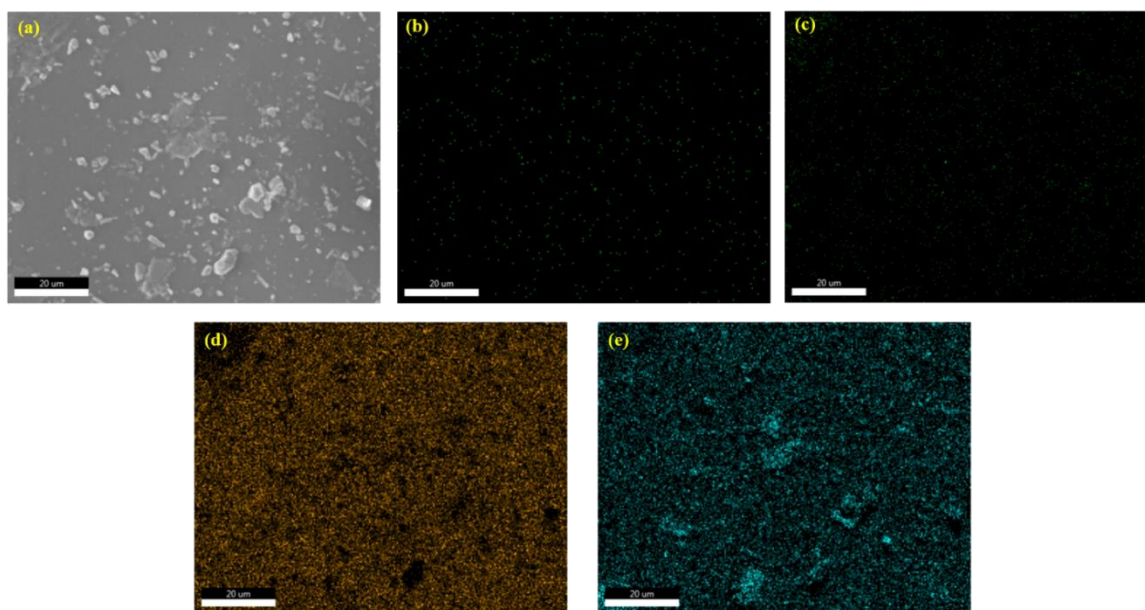


**Figure 5** (a) SEM image of BN1 nanocomposite; Elemental maps of (b) Boron (c) Nitrogen (d) Silicon (e) Oxygen

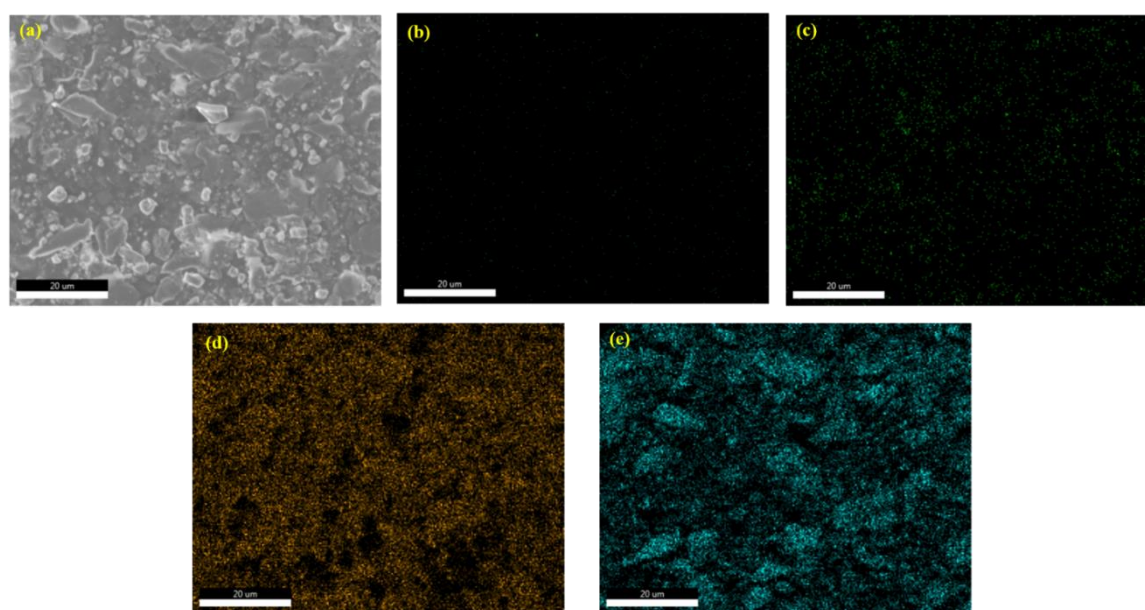


**Figure 6** (a) SEM image of BN2 nanocomposite; Elemental maps of (b) Boron (c) Nitrogen (d) Silicon (e) Oxygen

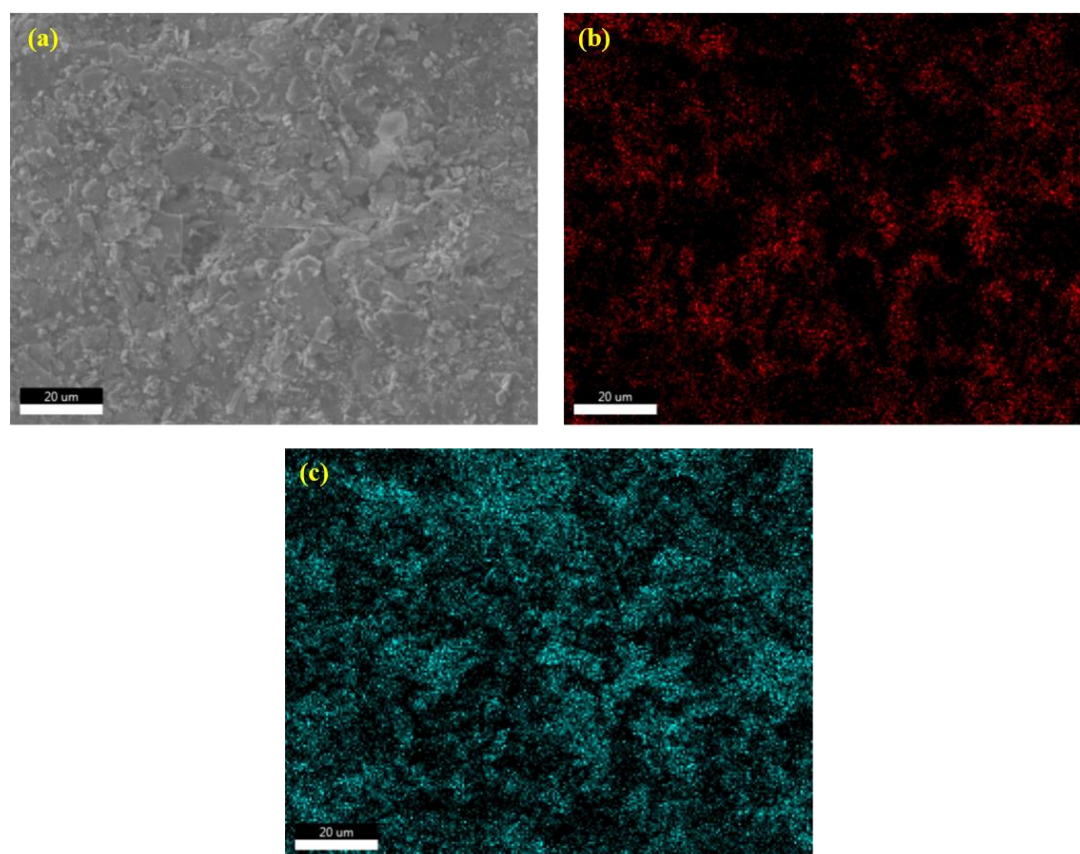


**Figure 7** (a) SEM image of nanocomposite electrode; Elemental maps of (b) Carbon (c) Oxygen

#### 4.2 Tensile Tests

Tensile test samples were placed accordingly in the UTM and load was applied at 100mm/min. In Fig. 8(a-c), the stress-strain plots of pure resin sample, PDMS with 2.5 wt. % hBN, and 5 wt. % hBN are shown. There is a considerable increase in Young's modulus of PDMS after the addition of hBN fillers. This was determined from the slope of the plot. The elastic modulus of pure PDMS was found to be 0.297 MPa. After the addition of 2.5 wt. % hBN, modulus increased to 0.344 MPa and the addition of 5 wt. % hBN increased it to 0.535 MPa. The tensile strength of pure PDMS was found to be 0.563 MPa however, there was only a marginal increase in tensile strength after the addition of hBN to the polymer, they were 0.573 MPa and 0.581 MPa respectively. From this, it is clear that hBN contributes to the stiffness of the composite but not to the overall strength of the material.

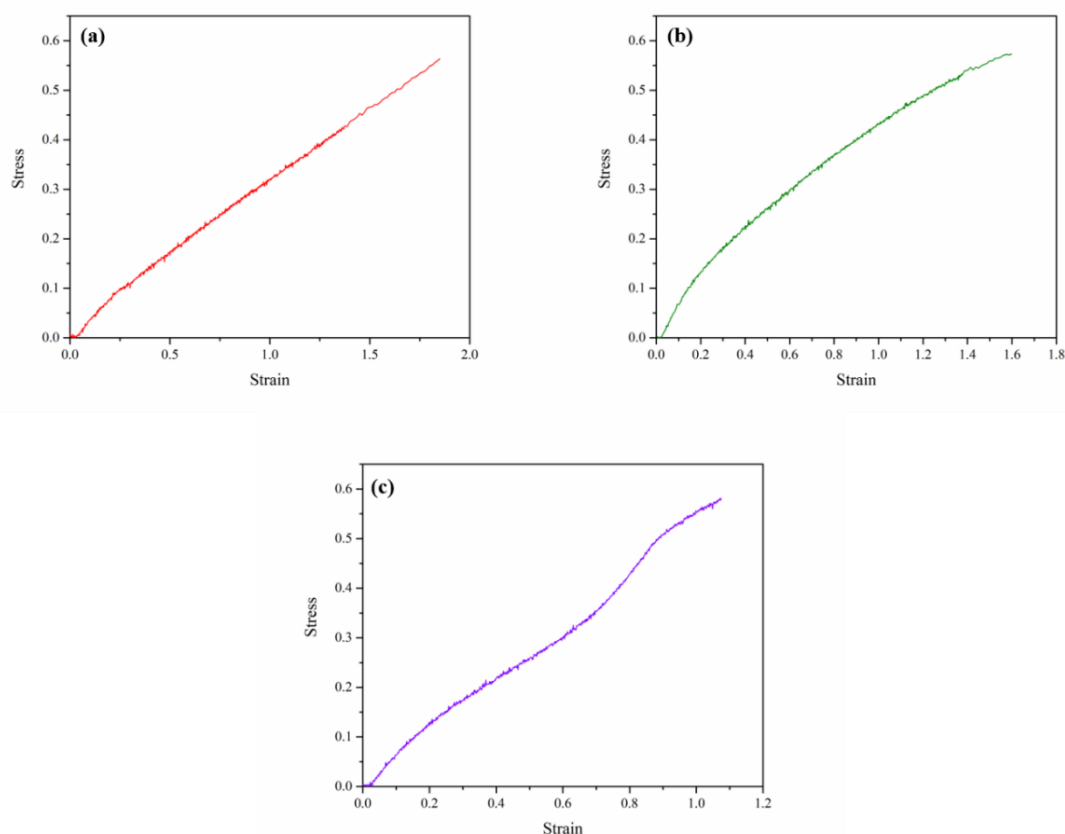


**Figure 8** Stress-Strain plots of (a) pure PDMS (b) 2.5 wt. % hBN-PDMS (c) 5 wt. % hBN-

### 4.3 Dielectric Permittivity

Dielectric constant or permittivity is an important factor for DEAs. Pure PDMS has a dielectric permittivity of 2.4<sup>71</sup>. The dielectric permittivity for the BN2 actuator at 20 Hz was found to be 3.33.

### 4.4 Actuator Testing

All four actuator types were connected to the DC power supply. Table 1 gives the actuation voltage required for each actuator type. When the voltage was increased beyond 5 kV for R1, there was a prominent displacement, and the actuator began to throb and stretch, and this confirms that EAPs have large strains. As the voltage gradually increased, the material lost its flexibility and became rigid. In BN1, there was a gradual increase in the stiffness of the material. This stiffness was more noticeable in the BN2 actuator and was due to the greater amount of hBN present in it. The thickness of each actuator was found to be 0.2 mm. For actuator BD\* the voltage was increased until the breakdown, which was 16 kV. The circuit shorted out with a bright spark at this stage.

Irrespective of the shape of the nanocomposite actuators, all of them showed small displacements only. These small displacements were found to be occurring around the edges of the electrodes, which then translated to the entire surface of the actuator making it stiff. Such small actuations would be useful in areas such as microfluidics.

**Table 1: Actuator test results**

Actuator Designation	Actuator Type	Observation	Actuation Voltage	Remark
R1	PDMS resin only	No visible crinkling, material stuck to the non-conductive sheet	5 kV	No filler
BN1	Composite- 2.5 wt. % hBN	Crinkling around electrode edges	8 kV	To study the influence of hBN in the actuator
BN2	Composite- 5 wt. % hBN	At 14 kV the actuator became stiff, and crinkling was more prominent	14 kV	Higher filler content requires higher actuation voltage
BD*	Composite- 5 wt. % hBN	A bright spark was seen, meaning that the circuit shorted out	16 kV	To demonstrate breakdown strength of actuator material

#### 4.5 FEA Simulations

For FEA simulations, the properties of the BN2 actuator were used. A micropump diaphragm model was simulated in COMSOL Multiphysics 5.5. All the 3D model components including electrodes were designed in Solidworks 2014. Two electrodes of different diameters were designed. The larger diameter electrode applies greater pressure on the actuator material, this design would aid in pumping the fluids. The diaphragm model used here is similar to the one which is found in conventional diaphragm pumps<sup>72</sup>. Then these models were imported into the COMSOL Multiphysics interface. The Physics setting chosen for solving the models were Solid Mechanics and Electrostatics, under the Stationary study setting. Solid Mechanics study was used to analyze the stresses and deformations that arise in the actuator when the voltage is applied. Electrostatics is the primary physics interface that drives the actuator. It provides the necessary mathematical functions that help in achieving the electromechanical coupling, which causes voltage-induced actuations. A fixed constraint was applied to the base of the model.

In Figure 9 (a-b), the proposed design of the micropump is shown. Figure 9(a) shows the micropump in an isometric view. Out of the two electrodes used, one was significantly larger than the other, the electrodes' dimensions are given in Table 2. Both electrodes were placed radially at the center of the elastomer. A larger top electrode was used in the diaphragm for creating a higher pressure for an effective pumping process. Here both inlet and outlet of the pump are shown. A non-return valve is required at the inlet to prevent any backflow. In Figure 9 (b), the same micropump is shown in the front view.

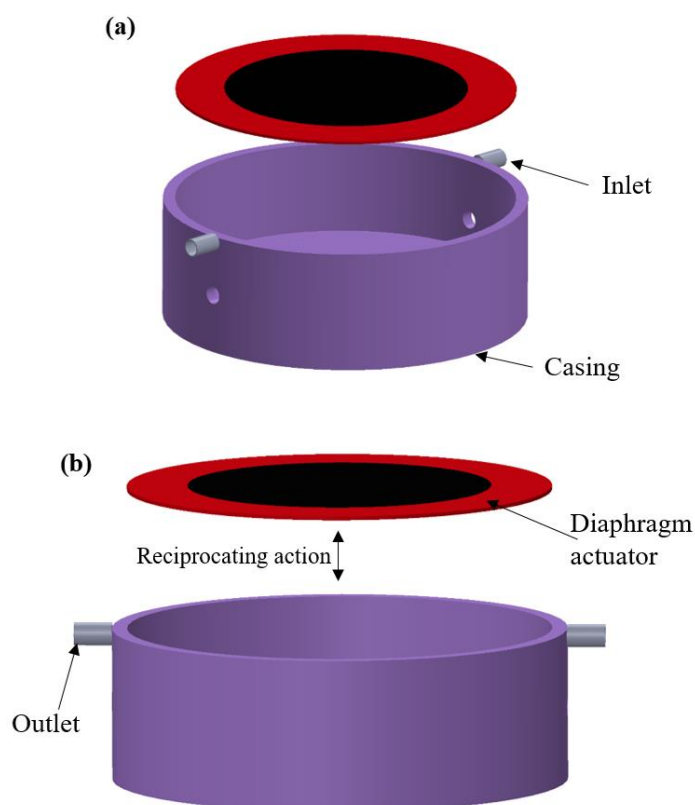


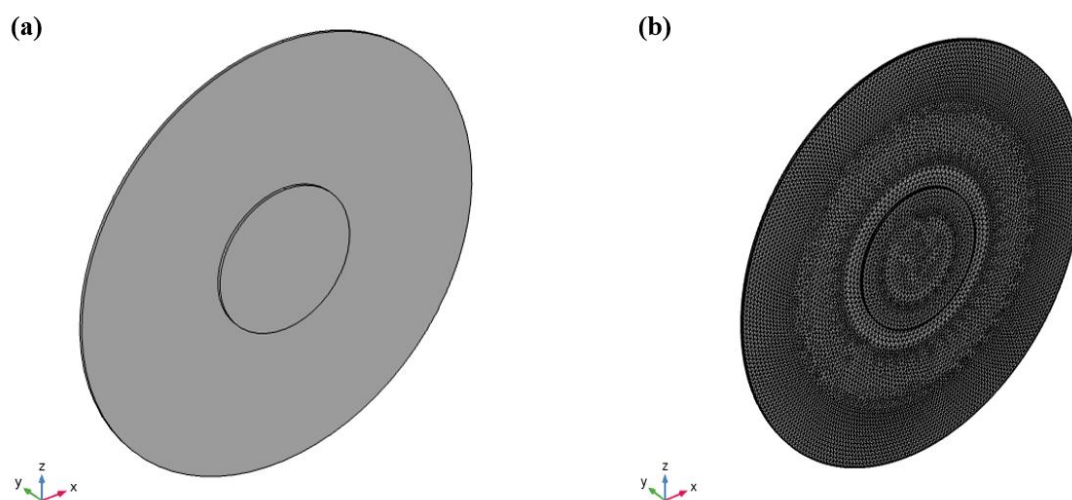
**Figure 9** Design of micropump (a) isometric view (b) front view

In Table 2 the model and mesh details are given. The 3D model of the micropump diaphragm was scaled down by half to obtain rapid FEA results.

**Table 2: FEA model specifications**

Description	Diaphragm membrane values
Actuator dimensions	Diameter= 3.0 cm Thickness= 0.02 cm
Top electrode dimension	Diameter= 1.6 cm Thickness= 0.01 cm
Bottom electrode dimension	Diameter= 1.0 cm Thickness= 0.01 cm
Mesh size	Fine (0.03 cm)
Actuation Voltage	14 kV

In Figure 10(a-b), the model and mesh of the diaphragm actuator are shown. The minimum mesh size was set at 0.03 cm for the diaphragm model. As the mesh size decreases, the results obtained become very accurate. In Table 3 the composite material properties are given. These properties were used to simulate the diaphragm actuator.

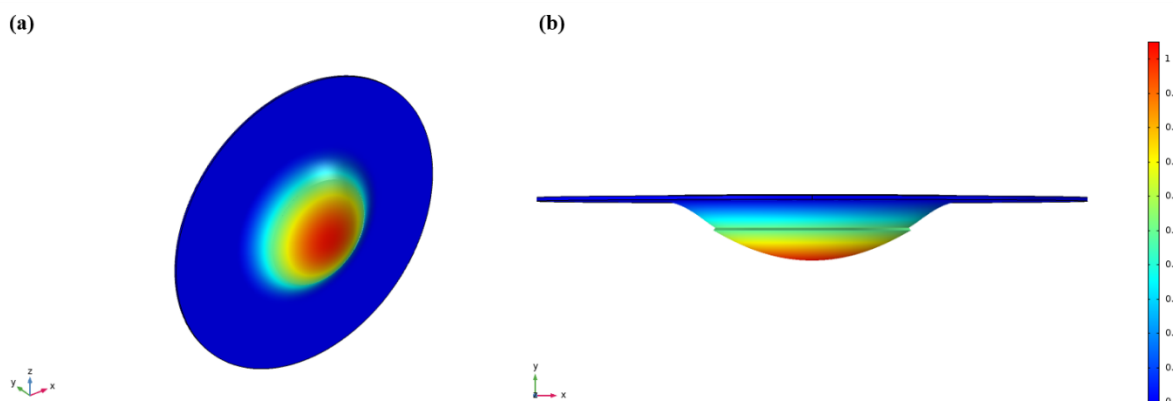


**Figure 10** Diaphragm actuator (a) 3D model (b) Meshed model, mesh size=0.03 cm

**Table 3: Material properties of 5 wt. % hBN-PDMS nanocomposite**

Description	Experimental Value
Density	970 kg/m <sup>3</sup>
Relative permittivity	3.33
Young's Modulus	0.535 MPa
Poisson's Ratio	0.48

For the applied voltage of 14 kV, the maximum displacement was 1.05 mm and the displacement result is given in Fig. 11(a-b). The resulting displacement generated by the model is small but this was what was expected from the material, as this tiny motion would perfectly handle the transport of microfluids without any loss. It is important to note the displacement occurs only in the active area of the nanocomposite.

**Figure 11** Displacement of the diaphragm actuator in (a) isometric view (b) side view; scale in mm

In Fig. 12, the cross-section of the diaphragm actuator is shown. In this result, the deformation in the electrodes and hBN- PDMS nanocomposite membrane can be seen. The plot gives the maximum displacement, which is in the active area.

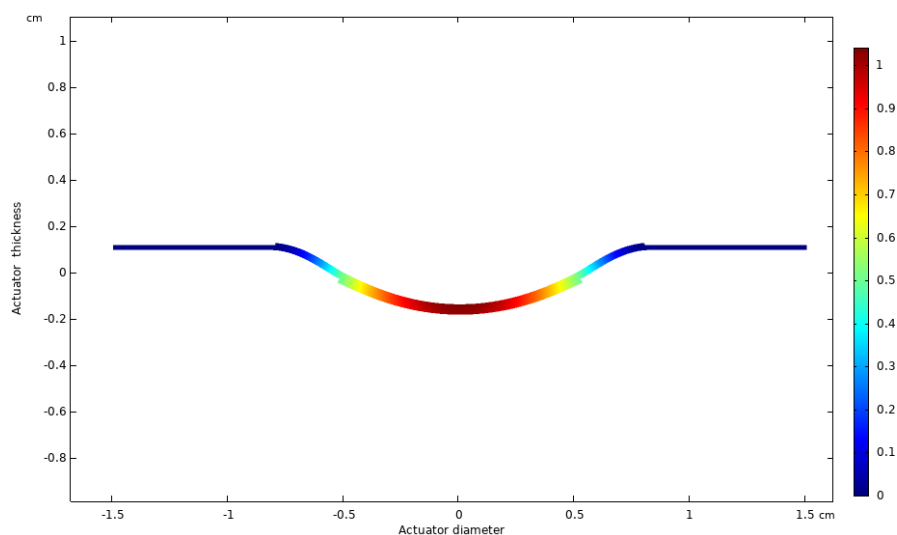


**Figure 12** Cross section of diaphragm actuator

In Fig. 13, the displacement of the actuator is plotted against the voltage applied. As the voltage gradually increases from 0 kV to 14 kV, the opposing electrodes compress the material thereby deforming it.

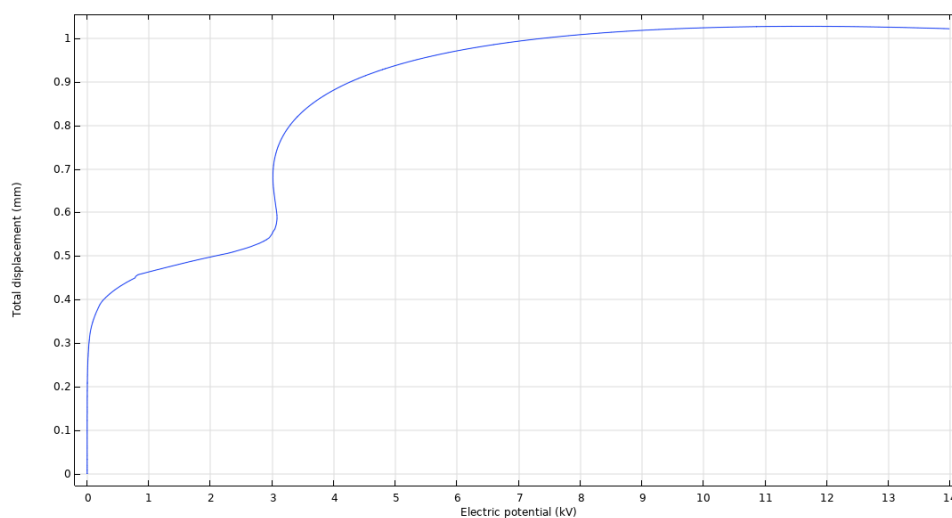


**Figure 13** Displacement vs Applied Voltage

The actuator has a maximum displacement of 1.05 mm at 14 kV, beyond which it fails as observed from the experiments. At 3 kV, there is a considerable jump in displacement, it could be said that this is the threshold point, here the Maxwell stress generated is very high and the electrodes begin to compress the hBN-PDMS actuator. From 3kV to 7 kV, there is an increase of 0.1 mm per kV. At 8 kV, the displacement is 1 mm, beyond which it begins to saturate and at 14 kV has a displacement of

1.05 mm. Thus, this plot gives the operating voltage for the designed actuator, which is 8 kV. Beyond 8 kV, the plot becomes linear. This is a confirmation that a smooth operation can be expected out of this device.

In Fig. 14(a-c), the von Mises stress generated in the actuator is given along with the energy density of the nanocomposite and voltage distribution in the model. The maximum stress generated was  $2.5 \times 10^4$  N/m<sup>2</sup> near the electrode of the actuator. The energy density of the actuator is  $2.5$  J/m<sup>3</sup> and is concentrated near the electrode areas, implying that the actuator is a capacitive device. Figure 14 (c) gives the voltage corresponding to its displacements and this appears as a range of different voltages acting on the electrode however, it is the voltage distribution corresponding to the displacement in the actuator. It gives a positional representation of the voltage on the electrode and this can be interpreted with Figures 12 & 13. It is to be noted that only at a certain voltage a particular displacement is obtained.

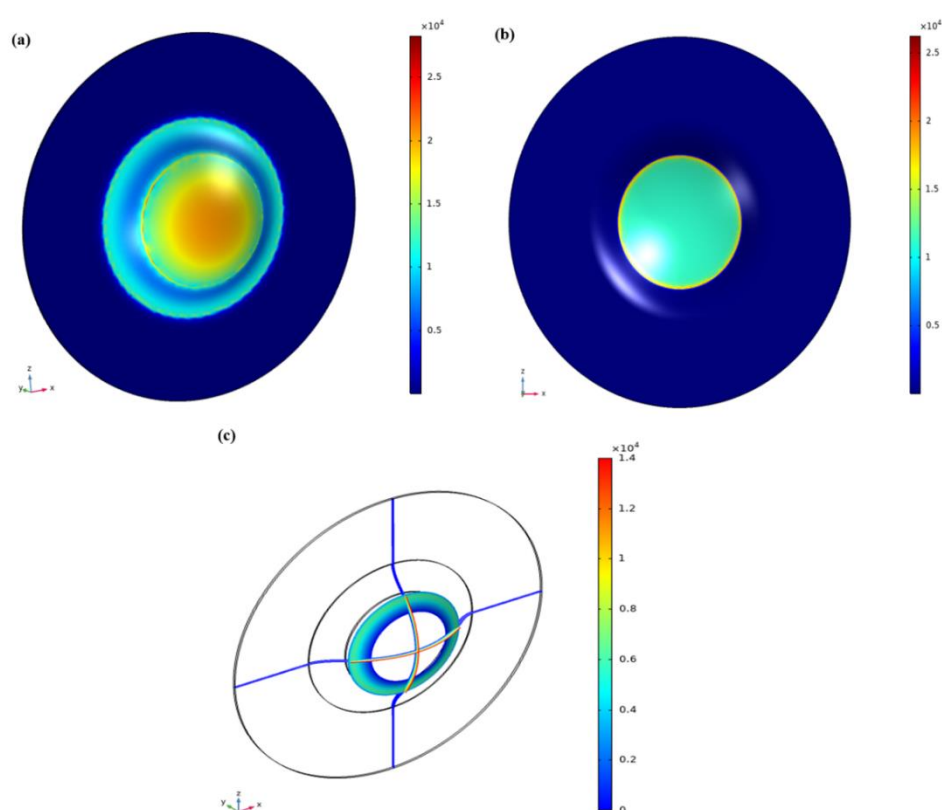


**Figure 14** Important parameters of the actuator (a) von Mises stress (b) energy density (c) voltage distribution

From equation (1), the Maxwell's stress generated for an applied voltage of 14 kV was calculated to be 144.5 kPa. The elastic modulus of the 5 wt. % hBN-PDMS nanocomposite was experimentally determined to be 535 kPa. In this case, to obtain 100 % deformation or more, Maxwell's stress generated should be three times greater than the elastic modulus of the nanocomposite. However, due to the higher material stiffness, the deformation made by the actuator is very small. This increase in material stiffness was achieved by the addition of hexagonal boron nitride nanoparticles to the PDMS matrix. Therefore, the nanofiller increases the modulus of the material thus making it stiffer, but beyond 5 wt. % the composite would behave like a resistor and would not be able to produce any actuations.

## 5. Conclusion

The need for precision actuators ranges from simple microfluidic devices to complex space telescopes. Though the mechanism of actuation would differ, the resultant displacement produced is in the range of nanometers to microns. This paper deals with such an actuator that is capable of producing actuations in the millimeter range. This actuator works based on dielectric elastomeric actuator technology. These typically large straining actuators were made to bring about small actuations by adding Boron Nitride nanofillers to the dielectric elastomer.

Experimental and simulation studies were carried out for the hBN-PDMS nanocomposite actuators. There was no large-scale deformation in the nanocomposite actuator, only small visible actuations or displacements were seen. Based on the studies, we conclude that the addition of particulate dielectric fillers to a polymer matrix could bring about small controllable actuations, achieved by increasing the stiffness of a material. The addition of hBN fillers to PDMS altered the overall stiffness of the nanocomposite. This is evident from the increase in Young's modulus of the nanocomposites. FEA simulation carried out for the BN2 nanocomposite-based diaphragm showed that a very small displacement of 1 mm could be achieved. On comparing this displacement with the thickness of the diaphragm actuator, which was 0.2 mm, an overall displacement of around 80% was obtained. The operational voltage for the diaphragm actuator was 8 kV and is the same as the conventional operating

voltage of existing actuator technologies. Such actuator materials would help in controlled fluid transport where a lossless aqueous transfer is critical and in places where precise actuations are required.

The following inferences were made:

- The addition of hBN nanoparticles increased the permittivity of the actuator material.
- More importantly, the addition of hBN altered the stiffness of the EAP (electroactive polymer) by increasing the Young's modulus. This contributes to the decreased straining in the actuator.

Thus, we conclude that the fabricated dielectric nanocomposite actuator material would be suitable for fabricating lightweight and low straining pumping mechanisms for devices such as micropumps.

- The nanocomposite actuator would be useful to fabricate micropump mechanisms where minute volumes of liquids need to be transported such as lab-on-chip devices or high-performance liquid chromatography columns. Such small displacements would help in creating a linear flow and would prove highly efficient in automating the pumping process.

### **Acknowledgments**

Author Adithya Lenin would like to thank the Centre for Research, Anna University, Chennai for awarding the Anna Centenary Research Fellowship for carrying out the research.

### **Author Contributions**

Adithya Lenin- Planning, design, fabrication & experimental-simulation, writing; Pandurangan Arumugam- Supervision.

### **Competing Interest statement**

The authors do not have any competing interests to declare.

## References

- (1) Liu, L.; Zhang, Z.; Liu, Y.; Leng, J. Failure Modeling of Folded Dielectric Elastomer Actuator. *Sci. China Physics, Mech. Astron.* **2014**, *57* (2), 263–272. <https://doi.org/10.1007/s11433-013-5047-z>.
- (2) Del Cura, V. O.; Cunha, F. L.; Aguiar, M. L.; Cliquet, A. Study of the Different Types of Actuators and Mechanisms for Upper Limb Prostheses. *Artif. Organs* **2003**, *27* (6), 507–516. <https://doi.org/10.1046/j.1525-1594.2003.07000.x>.
- (3) Asadi Dereshgi, H.; Dal, H.; Sayan, M. E. Analytical Analysis of a Circular Unimorph Piezoelectric Actuator in the Range of Low Voltages and Pressures. *Microsyst. Technol.* **2020**, *26* (8), 2453–2464. <https://doi.org/10.1007/s00542-020-04786-w>.
- (4) Popa, D. Microactuators BT - Encyclopedia of Microfluidics and Nanofluidics; Li, D., Ed.; Springer US: Boston, MA, 2008; pp 1100–1103. [https://doi.org/10.1007/978-0-387-48998-8\\_891](https://doi.org/10.1007/978-0-387-48998-8_891).
- (5) Srikar, V. T.; Spearing, S. M. Materials Selection for Microfabricated Electrostatic Actuators. *Sensors Actuators A Phys.* **2003**, *102* (3), 279–285. [https://doi.org/https://doi.org/10.1016/S0924-4247\(02\)00393-X](https://doi.org/https://doi.org/10.1016/S0924-4247(02)00393-X).
- (6) Zhao, H.; Zhang, L.; Yang, M. H.; Dang, Z. M.; Bai, J. Temperature-Dependent Electro-Mechanical Actuation Sensitivity in Stiffness-Tunable BaTiO<sub>3</sub>/Polydimethylsiloxane Dielectric Elastomer Nanocomposites. *Appl. Phys. Lett.* **2015**, *106* (9), 2–7. <https://doi.org/10.1063/1.4914012>.
- (7) Shao, J.; Wang, J. W.; Wei, L.; Wu, S. Q.; Yang, Y. H.; Ren, H. A Novel High Dielectric Constant Acrylic Resin Elastomer Nanocomposite with Pendant Oligoanilines. *Compos. Part B Eng.* **2019**, *176* (June), 107216. <https://doi.org/10.1016/j.compositesb.2019.107216>.
- (8) Nam, J. D.; Choi, H. R.; Koo, J. C.; Lee, Y. K.; Kim, K. J. Dielectric Elastomers for Artificial Muscles. In *Electroactive Polymers for Robotic Applications: Artificial Muscles and Sensors*; 2007; pp 37–48. [https://doi.org/10.1007/978-1-84628-372-7\\_2](https://doi.org/10.1007/978-1-84628-372-7_2).
- (9) Yuan, X.; Changgeng, S.; Yan, G.; Zhenghong, Z. Application Review of Dielectric Electroactive Polymers (DEAPs) and Piezoelectric Materials for Vibration Energy Harvesting. *J. Phys. Conf. Ser.* **2016**, *744*, 12077. <https://doi.org/10.1088/1742-6596/744/1/012077>.
- (10) Kanaan, A. F.; Pinho, A. C.; Piedade, A. P. Electroactive Polymers Obtained by Conventional and Non-

- Conventional Technologies. *Polymers* . 2021. <https://doi.org/10.3390/polym13162713>.
- (11) Festin, N.; Plesse, C.; Chevrot, C.; Pirim, P.; Vidal, F. 8 - Conducting Interpenetrating Polymer Networks Actuators for Biomimetic Vision System. In *Woodhead Publishing Series in Electronic and Optical Materials*; Ngo, T. D. B. T.-B. T., Ed.; Woodhead Publishing, 2015; pp 163–179. <https://doi.org/https://doi.org/10.1016/B978-0-08-100249-0.00008-2>.
- (12) Cardoso, V. F.; Ribeiro, C.; Lanceros-Mendez, S. 3 - Metamorphic Biomaterials; Rodrigues, L., Mota, M. B. T.-B. M. for M. A., Eds.; Woodhead Publishing, 2017; pp 69–99. <https://doi.org/https://doi.org/10.1016/B978-0-08-100741-9.00003-6>.
- (13) Carpi, F.; Kornbluh, R.; Sommer-Larsen, P.; Alici, G. Electroactive Polymer Actuators as Artificial Muscles: Are They Ready for Bioinspired Applications? *Bioinspir. Biomim.* **2011**, *6* (4), 45006. <https://doi.org/10.1088/1748-3182/6/4/045006>.
- (14) Kruusamäe, K.; Punning, A.; Aabloo, A.; Asaka, K. Self-Sensing Ionic Polymer Actuators: A Review. *Actuators* . 2015. <https://doi.org/10.3390/act4010017>.
- (15) Vu-Cong, T.; Jean-Mistral, C.; Sylvestre, A. Impact of the Nature of the Compliant Electrodes on the Dielectric Constant of Acrylic and Silicone Electroactive Polymers. *Smart Mater. Struct.* **2012**, *21* (10), 105036–105046. <https://doi.org/10.1088/0964-1726/21/10/105036>.
- (16) O'Halloran, A.; O'Malley, F.; McHugh, P. A Review on Dielectric Elastomer Actuators, Technology, Applications, and Challenges. *J. Appl. Phys.* **2008**, *104* (7). <https://doi.org/10.1063/1.2981642>.
- (17) Mateiu, R. V; Yu, L.; Skov, A. L. Electrical Breakdown Phenomena of Dielectric Elastomers. In *Electroactive Polymer Actuators and Devices (EAPAD) 2017*; 2017; Vol. 10163, p 1016328. <https://doi.org/10.1117/12.2258719>.
- (18) Heng, K.; Ahmed, A. S.; Shrestha, M.; Lau, G. Strong Dielectric-Elastomer Grippers with Tension Arch Flexures. In *Electroactive Polymer Actuators and Devices (EAPAD) 2017*; 2017; Vol. 10163, p 101631Z. <https://doi.org/10.1117/12.2259926>.
- (19) Romasanta, L. J.; Lopez-Manchado, M. A.; Verdejo, R. Increasing the Performance of Dielectric Elastomer Actuators: A Review from the Materials Perspective. *Prog. Polym. Sci.* **2015**, *51*, 188–211. <https://doi.org/10.1016/j.progpolymsci.2015.08.002>.

- (20) Youn, J. H.; Jeong, S. M.; Hwang, G.; Kim, H.; Hyeon, K.; Park, J.; Kyung, K. U. Dielectric Elastomer Actuator for Soft Robotics Applications and Challenges. *Appl. Sci.* **2020**, *10* (2).  
<https://doi.org/10.3390/app10020640>.
- (21) Wissler, M.; Mazza, E.; Kovacs, G. Electromechanical Coupling in Cylindrical Dielectric Elastomer Actuators. *Electroact. Polym. Actuators Devices 2007* **2007**, 6524, 652409.  
<https://doi.org/10.1117/12.714946>.
- (22) Mohd Ghazali, F. A.; Mah, C. K.; AbuZaiter, A.; Chee, P. S.; Mohamed Ali, M. S. Soft Dielectric Elastomer Actuator Micropump. *Sensors Actuators, A Phys.* **2017**, *263*, 276–284.  
<https://doi.org/10.1016/j.sna.2017.06.018>.
- (23) Bar-Cohen, D. Y. Electroactive Polymers as Artificial Muscles – Reality and Challenges Yoseph Bar-Cohen NDEAA Technologies , JPL / Caltech , Pasadena , CA. *Proc. 42nd AIAA Struct. Struct. Dyn. Mater. Conf.* **2001**.
- (24) MacLeod, P. J.; Hamer, G. K.; Lukose, P.; Georges, M. K. *Functional Polymers*; 1998.  
<https://doi.org/10.1021/bk-1998-0704.ch003>.
- (25) Kleo, M.; Förster-Zügel, F.; Schlaak, H. F.; Wallmersperger, T. Thermo-Electro-Mechanical Behavior of Dielectric Elastomer Actuators: Experimental Investigations, Modeling and Simulation. *Smart Mater. Struct.* **2020**, *29* (8), 085001. <https://doi.org/10.1088/1361-665x/ab8a6b>.
- (26) Sommer-Larsen, P.; Hooker, J. C.; Kofod, G.; West, K.; Benslimane, M.; Gravesen, P. Response of Dielectric Elastomer Actuators. In *Smart Structures and Materials 2001: Electroactive Polymer Actuators and Devices*; 2003; Vol. 4329, p 157. <https://doi.org/10.1117/12.432641>.
- (27) Bar-Cohen, Y. Electroactive Polymers as an Enabling Materials Technology. *Proc. Inst. Mech. Eng. Part G J. Aerosp. Eng.* **2007**, *221* (4), 553–564. <https://doi.org/10.1243/09544100JAERO141>.
- (28) Cochrane, C.; Hertleer, C.; Schwarz-Pfeiffer, A. 2 - Smart Textiles in Health: An Overview. In *Woodhead Publishing Series in Textiles*; Koncar, V. B. T.-S. T. and their A., Ed.; Woodhead Publishing: Oxford, 2016; pp 9–32. <https://doi.org/https://doi.org/10.1016/B978-0-08-100574-3.00002-3>.
- (29) Ionescu, M.; Winton, B.; Wexler, D.; Siegele, R.; Deslantes, A.; Stelcer, E.; Atanacio, A.; Cohen, D. D.

- Enhanced Biocompatibility of PDMS (Polydimethylsiloxane) Polymer Films by Ion Irradiation. *Nucl. Instruments Methods Phys. Res. Sect. B Beam Interact. with Mater. Atoms* **2012**, *273*, 161–163.  
<https://doi.org/10.1016/j.nimb.2011.07.065>.
- (30) Courtney, J. M. Polymers in Medicine and Surgery. *Biomaterials* **2003**, *1* (1), 60.  
[https://doi.org/10.1016/0142-9612\(80\)90063-0](https://doi.org/10.1016/0142-9612(80)90063-0).
- (31) Lai, Y.; Bordatchev, E. V; Nikumb, S. K. Metallic Micro Displacement Capacitive Sensor Fabricated by Laser Micromachining Technology. *Microsyst. Technol.* **2006**, *12* (8), 778.  
<https://doi.org/10.1007/s00542-006-0151-x>.
- (32) Zhang, H.; Zhou, Y.; Dai, M.; Zhang, Z. A Novel Flying Robot System Driven by Dielectric Elastomer Balloon Actuators. *J. Intell. Mater. Syst. Struct.* **2018**, *29* (11), 2522–2527.  
<https://doi.org/10.1177/1045389X18770879>.
- (33) Liu, S.; Tian, M.; Zhang, L.; Lu, Y.; Chan, T. W.; Ning, N. Tailoring Dielectric Properties of Polymer Composites by Controlling Alignment of Carbon Nanotubes. *J. Mater. Sci.* **2016**, *51* (5), 2616–2626.  
<https://doi.org/10.1007/s10853-015-9575-y>.
- (34) Kumar, D.; Sarangi, S. Dynamic Modeling of a Dielectric Elastomeric Spherical Actuator: An Energy-Based Approach. *Soft Mater.* **2021**, *19* (2), 129–138. <https://doi.org/10.1080/1539445X.2019.1616557>.
- (35) Sommer-Larsen, P.; Kofod, G.; Shridhar, M. H.; Benslimane, M.; Gravesen, P. Performance of Dielectric Elastomer Actuators and Materials. In *Smart Structures and Materials 2002: Electroactive Polymer Actuators and Devices (EAPAD)*; 2002; Vol. 4695, pp 158–166.  
<https://doi.org/10.1117/12.475161>.
- (36) Ahn, C. H.; Allen, M. G. Fluid Micropumps Based on Rotary Magnetic Actuators. In *Proceedings IEEE Micro Electro Mechanical Systems. 1995*; 1995; p 408. <https://doi.org/10.1109/MEMSYS.1995.472590>.
- (37) Wang, Y.-N.; Fu, L.-M. Micropumps and Biomedical Applications – A Review. *Microelectron. Eng.* **2018**, *195*, 121–138. <https://doi.org/https://doi.org/10.1016/j.mee.2018.04.008>.
- (38) Yildirim, Y. A.; Toprak, A.; Tigli, O. Piezoelectric Membrane Actuators for Micropump Applications Using PVDF-TrFE. *J. Microelectromechanical Syst.* **2018**, *27* (1), 86–94.  
<https://doi.org/10.1109/JMEMS.2017.2773090>.

- (39) Wang, Y. N.; Fu, L. M. Micropumps and Biomedical Applications – A Review. *Microelectron. Eng.* **2018**, *195* (December 2017), 121–138. <https://doi.org/10.1016/j.mee.2018.04.008>.
- (40) Tetteh, E. A.; Boatemaa, M. A.; Martinson, E. O. A Review of Various Actuation Methods in Micropumps for Drug Delivery Applications. *Proc. 11th Int. Conf. Electron. Comput. Comput. ICECCO 2014* **2014**. <https://doi.org/10.1109/ICECCO.2014.6997540>.
- (41) Guo, S.; Asaka, K. New Type of Micropump Driven by a Low Electric Voltage. *Acta Mech. Sin. Xuebao* **2004**, *20* (2), 146–151. <https://doi.org/10.1007/bf02484258>.
- (42) Blanchard, D.; Ligrani, P.; Gale, B. Single-Disk and Double-Disk Viscous Micropumps. *Sensors Actuators A Phys.* **2005**, *122* (1), 149–158. <https://doi.org/https://doi.org/10.1016/j.sna.2005.03.072>.
- (43) Gupta, N. K.; Gianchandani, Y. B. A Planar Cascading Architecture for a Ceramic Knudsen Micropump. In *TRANSDUCERS 2009 - 2009 International Solid-State Sensors, Actuators and Microsystems Conference*; 2009; pp 2298–2301. <https://doi.org/10.1109/SENSOR.2009.5285895>.
- (44) Warden, R. M. Cryogenic Nano-Actuator for JWST. *38th Aerosp. Mech. Symposium* **2006**.
- (45) Chonis, T. S.; Gallagher, B. B.; Knight, J. S.; Acton, D. S.; Smith, K. Z.; Wolf, E.; Coppock, E.; Tersigni, J.; Comeau, T. Characterization and Calibration of the James Webb Space Telescope Mirror Actuators Fine Stage Motion. In *Proc.SPIE*; 2018; Vol. 10698. <https://doi.org/10.1117/12.2311815>.
- (46) Gale, B. K.; Jafek, A. R.; Lambert, C. J.; Goenner, B. L.; Moghimifam, H.; Nze, U. C.; Kamarapu, S. K. A Review of Current Methods in Microfluidic Device Fabrication and Future Commercialization Prospects. *Inventions* . 2018. <https://doi.org/10.3390/inventions3030060>.
- (47) Asadi Dereshgi, H.; Dal, H.; Yildiz, M. Z. Piezoelectric Micropumps: State of the Art Review. *Microsyst. Technol.* **2021**. <https://doi.org/10.1007/s00542-020-05190-0>.
- (48) Carpi, F.; De Rossi, D. Improvement of Electromechanical Actuating Performances of a Silicone Dielectric Elastomer by Dispersion of Titanium Dioxide Powder. *IEEE Trans. Dielectr. Electr. Insul.* **2005**, *12* (4), 835–843. <https://doi.org/10.1109/TDEI.2005.1511110>.
- (49) Cohen, Y. B. *Electroactive Polymer (EAP) Actuators as Artificial Muscles*; 2013; Vol. 2. <https://doi.org/10.1017/CBO9781107415324.004>.
- (50) Tagarielli, V. L.; Hildick-Smith, R.; Huber, J. E. Electro-Mechanical Properties and Electrostriction

- Response of a Rubbery Polymer for EAP Applications. *Int. J. Solids Struct.* **2012**, *49* (23–24), 3409–3415. <https://doi.org/10.1016/j.ijsolstr.2012.07.018>.
- (51) Kim, K. J.; Shahinpoor, M. Development of Three-Dimensional Polymeric Artificial Muscles. In *Smart Structures and Materials 2001: Electroactive Polymer Actuators and Devices*; 2003; Vol. 4329, p 223. <https://doi.org/10.1117/12.432650>.
- (52) Benslimane, M.; Gravesen, P.; Group, M. T.; Danfoss, A. S.; Nordborg, D.-; Sommer-larsen, P. Mechanical Props of Dielectric Elastomer Actuators with Smart Metallic Compliant Electrodes. **2002**, *4695*, 150–157.
- (53) Jones, R. W.; Wang, P.; Lassen, B.; Sarban, R. Dielectric Elastomers and Compliant Metal Electrode Technology. *Proc. Mediterr. Electrotech. Conf. - MELECON* **2010**, 368–373. <https://doi.org/10.1109/MELCON.2010.5476257>.
- (54) Kofod, G.; Kornbluh, R.; Pelrine, R.; Sommer-larsen, P. Actuation Response of Polyacrylate Dielectric Elastomers. *Smart Struct. Mater. 2001 Electroact. Polym. Actuators Devices* **2001**, *4329* (May 2012), 141–147.
- (55) Corbaci, M.; Walter, W.; Lamkin-Kennard, K. Implementation of Soft-Lithography Techniques for Fabrication of Bio-Inspired Multi-Layer Dielectric Elastomer Actuators with Interdigitated Mechanically Compliant Electrodes. *Actuators* . 2018. <https://doi.org/10.3390/act7040073>.
- (56) Li, W.-B.; Zhang, W.-M.; Zou, H.-X.; Peng, Z.-K.; Meng, G. Bioinspired Variable Stiffness Dielectric Elastomer Actuators with Large and Tunable Load Capacity. *Soft Robot.* **2019**, *6* (5), 631–643. <https://doi.org/10.1089/soro.2018.0046>.
- (57) Stoyanov, H.; Kollosche, M.; Risse, S.; McCarthy, D. N.; Kofod, G. Elastic Block Copolymer Nanocomposites with Controlled Interfacial Interactions for Artificial Muscles with Direct Voltage Control. *Soft Matter* **2011**, *7* (1), 194–202. <https://doi.org/10.1039/c0sm00715c>.
- (58) Kang, J. H.; Sauti, G.; Park, C.; Yamakov, V. I.; Wise, K. E.; Lowther, S. E.; Fay, C. C.; Thibeault, S. A.; Bryant, R. G. Multifunctional Electroactive Nanocomposites Based on Piezoelectric Boron Nitride Nanotubes. *ACS Nano* **2015**, *9* (12), 11942–11950. <https://doi.org/10.1021/acs.nano.5b04526>.
- (59) Köckritz, T.; Luther, R.; Paschew, G.; Jansen, I.; Richter, A.; Jost, O.; Schönecker, A.; Beyer, E. Full

- Polymer Dielectric Elastomeric Actuators (DEA) Functionalised with Carbon Nanotubes and High-K Ceramics. *Micromachines* **2016**, *7* (10), 1–15. <https://doi.org/10.3390/mi7100172>.
- (60) Huang, J. H.; Ding, D. Electromechanical Analysis for a Piezo-Optical Fiber Subjected to Harmonic Loading. *J. Appl. Phys.* **2007**, *102* (6). <https://doi.org/10.1063/1.2783951>.
- (61) Bar-Cohen, Y.; Sherrit, S.; Lih, S. Characterization of the Electromechanical Properties of EAP Materials. In *Smart Structures and Materials 2001: Electroactive Polymer Actuators and Devices*; 2003; Vol. 4329, p 319. <https://doi.org/10.1117/12.432663>.
- (62) Wissler, M.; Mazza, E. Electromechanical Coupling in Dielectric Elastomer Actuators. *Sensors Actuators, A Phys.* **2007**, *138* (2), 384–393. <https://doi.org/10.1016/j.sna.2007.05.029>.
- (63) Pelrine, R. E.; Kornbluh, R. D.; Joseph, J. P. Electrostriction of Polymer Dielectrics with Compliant Electrodes as a Means of Actuation. *Sensors Actuators, A Phys.* **1998**, *64* (1), 77–85. [https://doi.org/10.1016/S0924-4247\(97\)01657-9](https://doi.org/10.1016/S0924-4247(97)01657-9).
- (64) Park, C.; Kang, J. H.; Harrison, J. S.; Costen, R. C.; Lowther, S. E. Actuating Single Wall Carbon Nanotube–Polymer Composites: Intrinsic Unimorphs. *Adv. Mater.* **2008**, *20* (11), 2074–2079. <https://doi.org/10.1002/adma.200702566>.
- (65) Meijer, K.; Rosenthal, M. S.; Full, R. J. Muscle-like Actuators? A Comparison between Three Electroactive Polymers. In *Smart Structures and Materials 2001: Electroactive Polymer Actuators and Devices*; 2003; Vol. 4329, p 7. <https://doi.org/10.1117/12.432649>.
- (66) Jia, K.; Lu, T. Numerical Study on the Electromechanical Behavior of Dielectric Elastomer with the Influence of Surrounding Medium. *Int. J. Smart Nano Mater.* **2016**, *7* (1), 52–68. <https://doi.org/10.1080/19475411.2016.1170074>.
- (67) Mirfakhrai, T.; Madden, J. D. W.; Baughman, R. H. Polymer Artificial. *Mater. Today* **2007**, *10* (4), 30–38. [https://doi.org/10.1016/S1369-7021\(07\)70048-2](https://doi.org/10.1016/S1369-7021(07)70048-2).
- (68) Pelrine, R.; Kornbluh, R.; Pei, Q.; Joseph, J. High-Speed Electrically Actuated Elastomers with Strain Greater than 100%. *Science (80-. )*. **2000**, *287* (5454), 836–839. <https://doi.org/10.1126/science.287.5454.836>.
- (69) Pelrine, R.; Kornbluh, R.; Kofod, G. High-Strain Actuator Materials Based on Dielectric Elastomers.

- Adv. Mater.* **2000**, *12* (16), 1223–1225. [https://doi.org/https://doi.org/10.1002/1521-4095\(200008\)12:16<1223::AID-ADMA1223>3.0.CO;2-2](https://doi.org/https://doi.org/10.1002/1521-4095(200008)12:16<1223::AID-ADMA1223>3.0.CO;2-2).
- (70) Xu, J.; Dong, Y.; Jiang, Z.; Tang, L.; Chen, X.; Yao, Z.; Cao, K. Self-Healing High-Performance Dielectric Elastomer Actuator with Novel Liquid-Solid Interpenetrating Structure. *Compos. Part A Appl. Sci. Manuf.* **2021**, *149*, 106519. <https://doi.org/https://doi.org/10.1016/j.compositesa.2021.106519>.
- (71) Du, P.; Lin, X.; Zhang, X. Dielectric Constants of PDMS Nanocomposites Using Conducting Polymer Nanowires. In *2011 16th International Solid-State Sensors, Actuators and Microsystems Conference*; 2011; pp 645–648. <https://doi.org/10.1109/TRANSDUCERS.2011.5969789>.
- (72) Iverson, B. D.; Garimella, S. V. Recent Advances in Microscale Pumping Technologies: A Review and Evaluation. *Microfluid. Nanofluidics* **2008**, *5* (2), 145–174. <https://doi.org/10.1007/s10404-008-0266-8>.